A first-principles study of the catalytic mechanism of the dehydriding reaction of $LiNH_2$ through adding Ti catalysts*

Zhang Hui(张 辉)[a)†], Liu Gui-Li(刘贵立)[b)], Qi Ke-Zhen(戚克振)[a)],
Zhang Guo-Ying(张国英)[a)], Xiao Ming-Zhu(肖明珠)[a)], and Zhu Sheng-Long(朱圣龙)[c)]

[a)] *College of Physics Science and Technology, Shenyang Normal University, Shenyang* 110034, *China*
[b)] *College of Constructional Engineering, Shenyang University of Technology, Shenyang* 110023, *China*
[c)] *State Key Laboratory for Corrosion and Protection, Institute of Metal Research, Chinese Academy of Sciences, Shenyang* 110016, *China*

(Received 28 April 2009; revised manuscript received 26 September 2009)

Experiments on a ball milled mixture with a 1:1 molar ratio of $LiNH_2$ and LiH with a small amount (1 mol %) of Ti^{nano}, $TiCl_3$ and TiO_2^{nano} have revealed a superior catalytic effect on Li–N–H hydrogen storage materials. In the x-ray diffraction profiles, no trace of Ti^{nano}, $TiCl_3$ and TiO_2^{nano} was found in these doped composites, by which we deduced that Ti atoms enter $LiNH_2$ by partial element substitution. A first-principles plane-wave pseudopotential method based on density functional theory has been used to investigate the catalytic effects of Ti catalysts on the dehydrogenating properties of $LiNH_2$ system. The results show that Ti substitution can reduce the dehydrogenation reaction activation energy of $LiNH_2$ and improve the dehydrogenating properties of $LiNH_2$. Based on the analysis of the density of states and overlap populations for $LiNH_2$ before and after Ti substitution, it was found that the stability of the system of $LiNH_2$ is reduced, which originates from the increase of the valence electrons at the Fermi level (E_F) and the decrease of the highest occupied molecular orbital (HOMO)–lowest unoccupied molecular orbital (LUMO) gap (ΔE_{H-L}) near E_F. The catalytic effect of Ti on the dehydrogenating kinetics of $LiNH_2$ may be attributed to the reduction of average populations between N–H per unit bond length (nm^{-1}), which leads to the reduction of the chemical bond strength of N–H.

Keywords: $LiNH_2$, first-principles calculation, dehydrogenating properties, Ti catalytic mechanism

PACC: 8640K, 7115H

1. Introduction

Hydrogen storage is a critical issue in the use of hydrogen as an energy carrier. The requirement for high-capacity hydrogen storage systems delimits our attention only to lightweight materials, such as lithium-based hydrides. In 2002, Chen *et al.*[1] reported that Li_3N could store hydrogen up to 10.6 wt% by the following two-step reactions.

$$Li_3N + 2H_2 \leftrightarrow Li_2NH + LiH + H_2 \leftrightarrow LiNH_2 + 2LiH. \quad (1)$$

However, the application of Li_3N as a hydrogen storage medium is greatly hindered by its high operating temperature. The dehydrogenation reaction caused by the decomposition of $LiNH_2$ to Li_2NH (right-to-left direction of reaction) begins at approximately 423–473 K in vacuum,[1,2] and 550 K in argon.[3,4] These temperatures are still too high for fuel cell applications. Therefore, the destabilisation of $LiNH_2$ to decrease the dehydriding temperature is an important research direction.

The mechanical alloying of $LiNH_2$ and metal elements (for example, Fe, Co, Ni metal) or Ti and V chlorides as catalysts have been experimentally confirmed to be efficient methods to solve the high operating temperature problem. Ichikawa *et al.*[5,6] examined the basic properties of a ball milled mixture with a 1:1 molar ratio of $LiNH_2$ and LiH with a small amount (1 mol%) of additives, such as the Fe, Co, Ni metal, or Ti and V chlorides. The result indicates that the ball milled mixture with $TiCl_3$ additives shows superior hydrogen storage properties. Alloying Fe, Co, Ni did not show any obvious catalytic effect. Isobe *et al.*[7] investigated the catalytic effect of some different type Ti additives on dehydro-

*Project supported by the National High Technology Research & Development of China (Grant No. 2009AA05Z105), the National Natural Science Foundation of China (Grant No. 50671069), the Science Research Program of the Education Bureau of Liaoning Province of China (Grant Nos. 2008S345, 2008511 and 2007T165), and the Financial Support from Shenyang Normal University.
†Corresponding author. E-mail: huizhangking@sina.com
© 2010 Chinese Physical Society and IOP Publishing Ltd

genating properties for the Li–N–H system. The results indicated that the Ti^{nano}, $TiCl_3$ and TiO_2^{nano} doped composites exhibited a superior catalytic effect in decreasing the temperature of hydrogen desorption, but the additives Ti^{micro} and TiO_2^{micro} did not act as a suitable catalyst for dehydrogenating properties of $LiNH_2$+LiH, which exhibited worse hydrogen desorption properties and were similar to the sample without any additives. In the x-ray diffraction (XRD) patterns, no trace of Ti^{nano}, $TiCl_3$, and TiO_2^{nano} was found in these doped composites. These results suggested that Ti^{nano}, $TiCl_3$, and TiO_2^{nano} are highly dispersed in the nanoscale and act as an effective catalyst in the reaction of hydrogen desorption.

The disappearance of Ti is an important revelation to understand the catalytic mechanism of the nanoscale metal Ti and its compounds on $LiNH_2$. We predict that Li atoms have been partially substituted by Ti atoms in $LiNH_2$, because Ti has larger electronegativity and more power to attract electrons to form Ti–N bonds. In recent years, the first-principles methods has been applied to the design of new lightweight hydrogen storage materials on the atomic scale.[8−10] So in the present study, we put forward a model of $LiNH_2$ where some Li atoms are partially replaced by Ti atoms, and perform a first-principles calculation to investigate the catalytic mechanism.

2. The models and the computation method

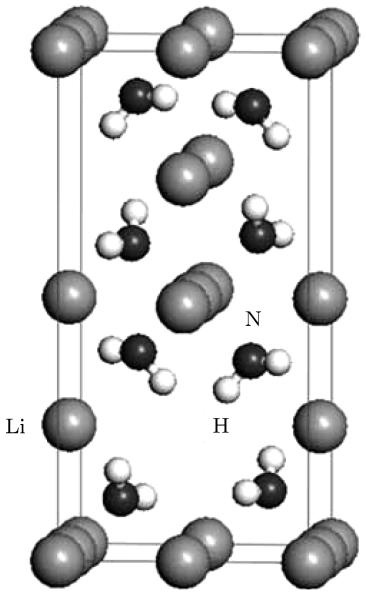
2.1. Crystal structure and models

The unit cells used for computation in the present work are shown in Fig. 1. The crystal structure of $LiNH_2$ is a body-centred tetragonal structure with space group $I\bar{4}$, where the lattice parameters are $a = b = 0.5037$ nm and $c = 1.0278$ nm, $\alpha = \beta = \gamma = 90°$.[11] There are eight formula units in a unit cell. The N atom is located at the $8g$ (0.2284, 0.2452, 0.1148) positions, and the two nonequivalent H atoms, here denoted as H1 and H2, are at the $8g$ (0.23, 0.15, 0.17) and (0.31, 0.36, 0.11) position, respectively. The Li atoms are at the $2a$ (0, 0, 0), $2c$ (0, 0.5, 0.25), and $4f$ (0, 0.5, 0.0042) positions, respectively. In the present work, we first calculate the total energy of $LiNH_2$ of the above structure with Ti substituting for Li at $2a$ (0, 0, 0), $2c$ (0, 0.5, 0.25), and $4f$ (0, 0.5, 0.0042) positions, and these results are listed in Table 1.

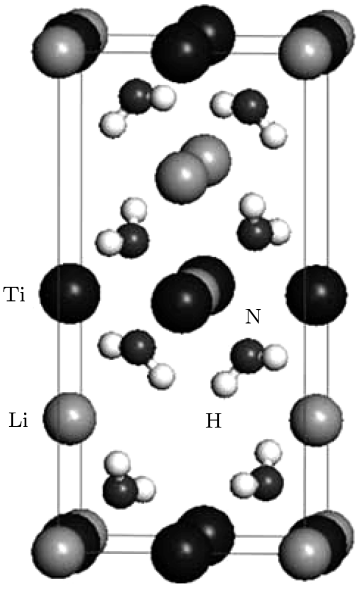
Table 1. Total energy of Li(Ti)NH_2.

substituting positions of Ti atoms	total energy of Li(Ti)NH_2/eV
$2a$ (0, 0, 0)	–6791.1792
$2c$ (0, 0.5, 0.25)	–6790.4489
$4f$ (0, 0.5, 0.0042)	–9617.7907

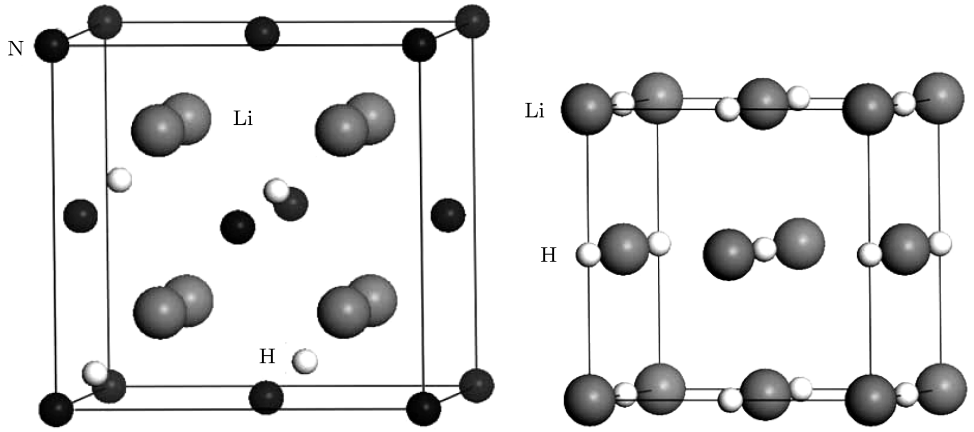
The total energy of $LiNH_2$ with Ti substituting positions at $4f$ (0, 0.5, 0.0042) is the lowest, which suggests that the system with $4f$ Li atoms substituted by Ti atoms is likely to be the most stable structure. Half of the Li atoms were substituted by Ti atoms. The crystal structures of $LiNH_2$ and Li(Ti)NH_2 are also shown in Fig. 1.



(a) $LiNH_2$



(b) Li(Ti)NH_2



(c) Li_2NH (d) LiH

Fig. 1. Crystal structures of $LiNH_2$ (a), $Li(Ti)NH_2$ (b), Li_2NH (c) and LiH (d).

The symmetry of crystalline Li_2NH is $F\bar{4}3m$, with a lattice parameter $a = 0.50769$ nm.[12] There are four formula units in one unit cell. The positions 4*c* (0.25, 0.25, 0.25) and 4*d* (0.75, 0.75, 0.75) are occupied by the Li atoms, and the 4*a* (0, 0, 0) positions by the N atom. The H atom prefers the 16*e* (0.093, 0.093, 0.093) positions. The H atom must partially occupy this position [Fig. 1(c)]. A quarter of the Li atoms are substituted by Ti atoms at 4*c* (0.25, 0.25, 0.25).

LiH is of NaCl crystal structure with a lattice parameter $a = 0.4037$ nm.

2.2. Methods

Cambridge Serial Total Energy Package (CASTEP),[13] a first-principles plane-wave pseudopotential method based on density functional theory (DFT) in which the exchange correlation potential adopts a generalised gradient approximation (GGA) of Perdew–Burke–Ernzerhof (PBE) form,[14,15] was used in this work. An ultra-soft pseudopotential presented in the reciprocal space with the Cepeley–Alder exchange–correlation potential[16] was used for all elements in our models. In our calculations, the cut-off energy of atomic wave functions (PWs) $E_{\rm cut}$ was set at 310 eV. Sampling of the irreducible wedge of the Brillouin zone used 4×4×2 with a regular Monkhorst–Pack grid of special *k*-points. A finite basis set correction[17] was applied for evaluation of energy and stress. In the calculation of self-consistent field (SCF), the Pulay scheme of density mixing[18] was adopted. All atomic positions in the present models have been relaxed according to the total energy and force using the Broyden–Flecher–Goldfarb–Shanno scheme[19] based on the cell optimisation criterion (root-mean-square (RMS) force of 0.03 eV/Å (1 Å=0.1 nm), RMS stress of 0.05 GPa, and RMS displacement of 1.0×10^{-3} Å). The calculation of total energy and electronic structure is followed by cell optimisation with SCF tolerance of 1.0×10^{-5} eV/atom under GGA–PBE potential respectively. The valence electron configurations of atoms are Li $2s^1$, N $2s^22p^3$, H $1s^1$, Ti $3d^24s^2$.

3. Results and discussion

3.1. Activation energy of dehydrogenation reaction

The reaction of hydride formation and hydride decomposition of $LiNH_2$ is described by expression (1). Frequently, hydrogenation is an exothermic reaction, while dehydrogenation is a reverse one. The reaction activation energy is the heat absorbed or released by the hydrogen storage system during hydrogenation or dehydrogenation. As far as the dehydrogenation process is concerned, less energy absorption means this hydrogen storage system can dehydrogenate easily. Thus, in order to understand the catalytic mechanism of Ti catalysts in the dehydrogenation reaction of $LiNH_2$, we define the reaction activation energy of

dehydrogenation [expression (1)] as follows:

$$\begin{aligned}\Delta Q1 &= \Sigma E_{\rm tot}(\text{products}) - \Sigma E_{\rm tot}(\text{reactants}) \\ &= E_{\rm tot}(\text{Li}_2\text{NH}) + E_{\rm tot}(\text{LiH}) + E_{\rm tot}(\text{H}_2) \\ &\quad - E_{\rm tot}(\text{LiNH}_2) - 2E_{\rm tot}(\text{LiH}). \end{aligned} \quad (2)$$

The dehydrogenation of Li(Ti)NH_2 follows the formula Li(Ti)NH_2+2LiH→Li(Ti)_2NH+LiH+H_2. The reaction activation energy of dehydrogenation for Li(Ti)NH_2 can be calculated by using the following equation

$$\begin{aligned}\Delta Q2 &= E_{\rm tot}[\text{Li(Ti)}_2\text{NH}] + E_{\rm tot}(\text{LiH}) + E_{\rm tot}(\text{H}_2) \\ &\quad - E_{\rm tot}[\text{Li(Ti)NH}_2] - 2E_{\rm tot}(\text{LiH}), \end{aligned} \quad (3)$$

where $E_{\rm tot}(\text{LiNH}_2)$, $E_{\rm tot}(\text{LiH})$, $E_{\rm tot}(\text{Li}_2\text{NH})$, $E_{\rm tot}[\text{Li(Ti)NH}_2]$ and $E_{\rm tot}[\text{Li}_2\text{(Ti)NH}]$ are the total energy of LiNH_2, LiH, Li_2NH, Li(Ti)NH_2 and Li_2(Ti)NH respectively. The total energy of the H_2 molecule $E_{\rm tot}(\text{H}_2)$ is determined by the optimisation of a 0.1 nm cube with H_2 at eight corners, and the bond length of H_2 is estimated as 0.0749 nm.

Table 2. Total energy and reaction activation energy of the systems considered (per formula unit).

systems	total energy/eV	activation energy ΔQ/kJ·mol^{-1}
LiNH_2	–495.9514	100.2909 (1.0395 eV)
Li(Ti)NH_2	–1202.2238	89.5334 (0.9280 eV)
LiH	–205.2530	—
Li_2NH	–668.4861	—
H_2	–31.6788	—
Li $(\text{Ti})_2$NH	–1374.8788	—

From Table 2, it is found that the dehydrogenation reaction activation energy of Li(Ti)NH_2 is about 10.7575 kJ/mol lower than that of LiNH_2, indicating that the existence of Ti catalysts makes the reaction of Li(Ti)NH_2+2LiH→Li_2(Ti)NH+LiH+H_2 easier to achieve than that of LiNH_2+2LiH→Li_2NH+LiH+H_2.

3.2. Electronic structure

Density of states is very useful for analysing the relationship between the electronic structure and the bonding of hydrogen storage compounds. Total and partial densities of states for LiNH_2 and Li(Ti)NH_2 are plotted in Figs. 2 and 3 to show the influence of Ti on the electronic structure of LiNH_2.

Figure 2 shows the total and partial densities of states (DOS) for LiNH_2. The total DOS shows three bonding peaks from −7.0 eV to Fermi energy. From −7.0 eV to −4.8 eV below the Fermi energy, these peaks are dominated by the bonding of Np with Hs electrons. In the intermediate region, from −3.0 eV to −1.8 eV below the Fermi energy, the bonding peaks contain all of the interactions among the three atoms, and show that the Li–N bonding is dominated by s–p and p–p interactions. From −1.2 eV to the Fermi energy, there are two peaks in the total DOS, which are contributed mainly by the Np, Lis and Lip electrons. There is a large energy band gap between $E_{\rm F}$ and 4.0 eV. The region below the energy band gap can be viewed as the valence band, and above which as the conduction band. These features indicate that LiNH_2 is nonmetallic.

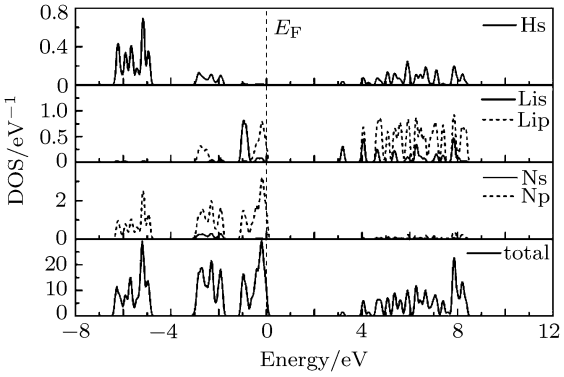


Fig. 2. Total and partial densities of states of LiNH_2.

Figure 3 shows the total DOS and partial DOS of Li(Ti)NH_2. This result was obtained by using the same cell as mentioned above but replacing $4f$ (0, 0.5,

0.0042) Li atoms with Ti atoms. From Fig. 3, it can be seen that the shape of the total DOS and partial DOS of $Li(Ti)NH_2$ is similar to that of $LiNH_2$; there are also three groups of bonding peaks. But because of the alloying with Ti, the bonding peaks of $Li(Ti)NH_2$ move toward the low energy region (from −6.5 eV–0 eV to −10.5 eV–−4.5 eV), and the Fermi energy level (E_F) is in the conduction band, so the system of $Li(Ti)NH_2$ becomes metal-like. The total DOS shows that three major bonding peaks focus on the energy region between −10.5 eV and −4.5 eV. Partial DOS analysis reveals that the bonding peak between −10.5 eV and −8.7 eV mainly originates from the contribution of Hs and Np electrons. The bonding peaks between −7.5 eV and −6 eV originate from the interaction of Hs, Np and Lip electrons. The bonding peaks between −5.5 eV and −4.5 eV result from the bonding of Lis, Lip and Np electrons.

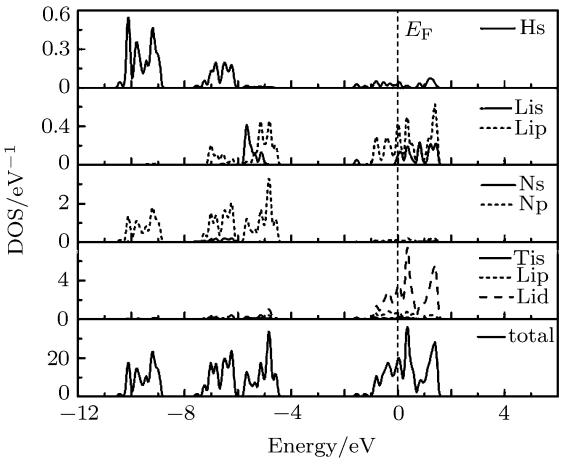


Fig. 3. Total and partial densities of states of $Li(Ti)NH_2$.

The valence electron number $N(E_F)$ at E_F and the HOMO–LUMO gap (ΔE_{H-L}) near E_F can be used to characterise and judge the structural stability of a crystal or cluster. The lower the $N(E_F)$,[20] or the bigger the ΔE_{H-L},[21] the higher the structural stability of crystals or clusters. Hence, the low structural stability of the $Li(Ti)NH_2$ system can be attributed to the increase in $N(E_F)$ and the decrease of the HOMO–LUMO gap to a value between −4.5 eV and −2.5 eV from (0.1 eV–4 eV). The low structural stability of the $Li(Ti)NH_2$ system as compared with the $LiNH_2$ phase indicates that the addition of Ti into $LiNH_2$ can accelerate the dehydrogenating kinetics of the $LiNH_2$ phase and reduce its decomposition temperature.

3.3. Mulliken overlap population

To further analyse the bonding characteristics, we take Table 3 to show the overlap population analysis for $LiNH_2$ and $Li(Ti)NH_2$. It can be seen from Table 3 that the average population between N–H is about 0.800 per unit bond length (nm^{-1}) for $LiNH_2$, indicating the bonding between N–H is strongly covalent. The average overlap population for N–H is 0.7423 per unit bond length (nm^{-1}) for $Li(Ti)NH_2$, which is slightly different from $LiNH_2$. The bond strength between N–H in $Li(Ti)NH_2$ is weaker than that in $LiNH_2$. After Ti substitution, the average overlap population between Li and N is increased to 0.1050 from 0.0950.

Table 3. Mulliken overlap population analysis for $LiNH_2$ and $Li(Ti)NH_2$.

systems	between Li and N	between H and N
$LiNH_2$	0.0950	0.8000
$Li(Ti)NH_2$	0.1050	0.7423

All these features indicate that Ti substitution reduces the bond strength between N–H. Therefore, from an electronic structure point of view, an explanation for the decreased dehydriding temperature of $LiNH_2$ is the weaker bonding of N–H in $Li(Ti)NH_2$. Also, we can assume that any catalyst or adulterant, if it can reduce the bond strength of N–H, is most likely a candidate catalyst to reduce the hydrogen desorption temperature of $LiNH_2$.

4. Conclusions

The catalytic mechanism of the Ti catalyst on the dehydriding reaction of $LiNH_2$ has been investigated by using a first-principles plane-wave pseudopotential method. Experiments using a ball milled mixture with a 1:1 molar ratio of $LiNH_2$ and LiH with a small amount (1 mol %) of Ti^{nano}, $TiCl_3$ or TiO_2^{nano} revealed that Ti atoms enter $LiNH_2$ by partial substitution. The dehydrogenation reaction activation energy and the electronic structures of $LiNH_2$ and $Li(Ti)NH_2$ were calculated. The results show that Ti substitution can reduce the dehydrogenation reaction activation energy of $LiNH_2$ and improve the dehydrogenating properties of $LiNH_2$. The low structural stability of the $Li(Ti)NH_2$ system as compared with $LiNH_2$ mainly originates from the increase of its valence electrons at the Fermi level $N(E_F)$ and the decrease of

the HOMO–LUMO gap ($\Delta E_{\mathrm{H-L}}$) near E_{F} caused by Ti substitution. The catalytic effect of Ti substitution on the dehydrogenating kinetics of $LiNH_2$ may be attributed to the weakening of the chemical bond strength of N–H, which leads to the decrease of the dehydrogenating temperature of $LiNH_2$.

References

[1] Chen P, Xiong Z T, Luo J Z, Lin J Y and Tan K L 2002 *Nature* **420** 302

[2] Orimo S, Nakamori Y, Kitahara G, Miwa K, Ohba N, Noritake T and Towata S 2004 *Appl. Phys.* A **79** 1765

[3] Nakamori Y and Orimo S 2004 *J. Alloys Compd.* **370** 271

[4] Nakamori Y and Orimo S 2004 *Mater. Sci. Eng.* B **108** 48

[5] Ichikawa T, Hanada N, Isob S, Leng H Y and Fujii H 2005 *J. Alloys. Compd.* **404** 435

[6] Ichikawa T, Isobe S, Hanada N and Fujii H 2004 *J. Alloys. Compd.* **365** 271

[7] Isob S, Ichikawa T and Hanada N 2005 *J. Alloys Compd.* **404** 439

[8] Zhou J J, Chen Y G, Wu G L, Zheng X, Fang Y C and Gao T 2009 *Acta Phys. Sin.* **58** 4853 (in Chinese)

[9] Chen Y H, Kang L, Zhang C R, Luo L C and Ma J 2008 *Acta Phys. Sin.* **57** 4866 (in Chinese)

[10] Chen Y H, Kang L, Zhang C R, Luo L C and Pu Z S 2008 *Acta Phys. Sin.* **57** 4174 (in Chinese)

[11] Song Y and Guo Z X 2006 *Phys. Rev.* B **74** 195120

[12] Ohoyama K, Nakamori Y, Orimo S and Yamada K 2005 *J. Phys. Soc. Jpn.* **74** 483

[13] Segall M D, Lindan P L D, Probert M J, Pickard C J, Hasinp P J, Clark S J and Payne M C 2002 *J. Phys. Condens. Matter* **14** 2717

[14] Marlo M and Milman V 2000 *Phys. Rev.* B **62** 2899

[15] Liu Z M, Cui T, Ma Y M, Liu B B and Zou G T 2007 *Acta Phys. Sin.* **56** 8 (in Chinese)

[16] Vanderbilt D 1990 *Phys. Rev.* B **41** 7892

[17] Franscis G P and Payne M C 1990 *J. Phys. Condens. Matter* **2** 4395

[18] Hammer B, Hansen L B and Norkov J K 1999 *Phys. Rev.* B **59** 7413

[19] Monkhorst H J and Pack J D 1976 *Phys. Rev.* B **13** 5188

[20] Imai Y, Mukaida M and Tsunoda T 2000 *Intermetallics* **8** 381

[21] Wang J, Wang G and Zhao J 2002 *Phys. Rev.* B **66** 035418